International Journal of Engineering, Mathematical and Physical Sciences
ISSN: 2517-9934
Vol:11, No:8, 2017

Methods for Material and Process Monitoring by Characterization of (Second and Third Order) Elastic Properties with Lamb Waves

R. Meier, M. Pander

***Abstract*—**In accordance with the industry 4.0 concept, manufacturing process steps as well as the materials themselves are going to be more and more digitalized within the next years. The "digital twin" representing the simulated and measured dataset of the (semi-finished) product can be used to control and optimize the individual processing steps and help to reduce costs and expenditure of time in product development, manufacturing, and recycling. In the present work, two material characterization methods based on Lamb waves were evaluated and compared. For demonstration purpose, both methods were shown at a standard industrial product - copper ribbons, often used in photovoltaic modules as well as in high-current microelectronic devices. By numerical approximation of the Rayleigh-Lamb dispersion model on measured phase velocities second order elastic constants (Young's modulus, Poisson's ratio) were determined. Furthermore, the effective third order elastic constants were evaluated by applying elastic, "non-destructive", mechanical stress on the samples. In this way, small microstructural variations due to mechanical preconditioning could be detected for the first time. Both methods were compared with respect to precision and inline application capabilities. Microstructure of the samples was systematically varied by mechanical loading and annealing. Changes in the elastic ultrasound transport properties were correlated with results from microstructural analysis and mechanical testing. In summary, monitoring the elastic material properties of plate-like structures using Lamb waves is valuable for inline and non-destructive material characterization and manufacturing process control. Second order elastic constants analysis is robust over wide environmental and sample conditions, whereas the effective third order elastic constants highly increase the sensitivity with respect to small microstructural changes. Both Lamb wave based characterization methods are fitting perfectly into the industry 4.0 concept.

***Keywords*—**Lamb waves, industry 4.0, process control, elasticity, acoustoelasticity.

I. Introduction

A. Solar Cell Interconnectors and their Influence on Solar Module Reliability

SOLAR cell interconnectors are tinned copper ribbons used for establishing the electrical interconnection of individual solar cells to solar cell strings (Fig. 1). The soldering process of these ribbons to solar cells is a critical step in solar module production. During soldering significant mechanical stresses are generated in the stringed cell assembly resulting from mismatch in thermal expansion of the individual interconnected materials. After cooling below the eutectic point of the solder (e.g. 183°C for Sn63Pb37) the cell interconnector determines the thermo-mechanical loading characteristics of the silicon cells. The interconnector consists of a quasi-rectangular shaped copper core surrounded with solder (such as Sn63Pb37 or Sn96.5Ag3.5) and is therefore often called copper ribbon. It has a six times larger coefficient of thermal expansion than silicon of the solar cells and is coupled to these by a thin layer of solder (thickness of 15-30 µm). Further cooling generates stresses, which load the ribbon, the solder and the silicon cell. These intrinsic stresses are acting on existing defects (micro-cracks) and superpose with stresses in further process steps. This way cracks can extend in further thermal (lamination, day/night, sun/shadow, resistivity losses) or mechanical (wind, snow) loading cycles and lead to sudden or delayed cell breakage. Broken cell pieces are moving within the module during thermal cycles. This may result in electrically isolated cell parts or cell shunting. In both cases the module efficiency is significantly reduced.

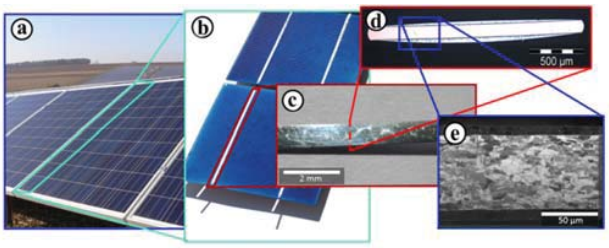

Fig. 1 (a) Solar modules in a solar field, (b) Solar cell string (inter-connected solar cells), (c) Cell interconnector, (d) Interconnector cross-section (light microscopy), (e) Grain structure of cross-section (scanning electron microscopy)

It can be prevented if the mechanical properties of the ribbon are well adjusted. In that case most of the generated stress is relieved by plastic deformation of the copper ribbon and solder layer thus the silicon is prevented from breakage. The mechanical properties of the ribbon are directly related to their microstructure and determined by the ribbon production process and subsequent loading conditions. For fast process optimization capabilities, as well as for achieving high continuous quality, inline material characterization methods have to be developed.

R. Meier is with Fraunhofer Institute for Microstructure of Materials and Systems IMWS, Halle (Saale), 06120 Germany (e-mail: rico.meier@imws.fraunhofer.de).

Ultrasonic methods are widely accepted methods for process control in many parts of industry. Unluckily the geometry of the interconnector (thickness < 0.2 mm) combined with high attenuation of high-frequent ultrasound in copper and the high production speeds (up to 30 m/s) make conventional ultrasonic testing methods based on volume waves not applicable, since the investigated sample length within one measurement is limited by the size of the transducer (or transducer array). Unrealistically high acquisition speeds would be needed for continuous measurements at full production speed. A solution could be the usage of low frequent guided waves (Lamb waves) traveling along the ribbon with wave speeds of several km/s. Lamb wave measurements allow a characterization of several meters of the ribbon within one measurement. Therefore, much fewer measurements are needed for continuous characterization.

B. State of Research

Elastic constant determination with volume waves is widely spread in industry [1]. Young's modulus Y and Poison's ratio ν of isotropic material are calculated from longitudinal c_L and transverse c_T wave velocities by:

$$Y = 2\rho\, c_T^2(1+\nu) \quad \text{and} \quad \nu = \frac{1-2\left(\frac{c_L}{c_T}\right)^2}{2-2\left(\frac{c_L}{c_T}\right)^2}, \tag{1}$$

where thickness D and density ρ of the sample are known.

As previously mentioned volume waves cannot be used due to the given characteristics of the samples and the desired production speed.

The velocity of Lamb waves does not only depend on geometry, density and elastic parameters, but also on frequency. This dispersive behavior was predicted by Horace Lamb in 1917 [2]. The dispersion relations can be calculated numerically in dependence of sample thickness and elastic parameters [3]-[5]. Even commercial software is available [6], [7]. Rogers determined the elastic constants by measuring the Lamb wave dispersion relations and fitting the numerical model on the measured wave speeds (inverse problem) [4]. Vignesh correlated the evaluated elastic constants to results from mechanical testing [8]. In this work the approach of Rogers will be further developed into a dispersion-based elastic constant characterization tool.

Another approach for ribbon characterization is based on acoustoelasticity – a third order elastic effect. Acoustoelasticity describes the variation of wave speed if the sound transmitting material is mechanically stressed. The theory of acoustoelasticity reaches back to Hughes and Kelly [9] and the theory of finite strains from Murnaghan [10]. It was further developed by Toupin and Bernstein [11], who described the elastic properties of stressed isotropic bodies with help of five constants. Important work in the field of acoustoelastic effects on guided waves were carried out at the University of Leipzig in the group of Professor Wolfgang Grill [13]-[15] and at the Georgia Institute of Technology in the group of the Professors Jennifer and Thomas Michaels [12], [16]. Muir investigated the influence of acoustoelasticity on volume waves traveling at an oblique angle through thick plates [12]. Furthermore he derived the acoustoelastic constant of a polycrystal by single crystal approximation. At the same time we investigated the influence of mechanical stresses generated by elastic and plastic deformation and temperature on volume and guide waves in cylindrical rods [13]. Tarar showed analytically that geometrical effects overlay the measured acoustoelasticity [14]. Amjad used the developed acoustoelastic methods to investigate acoustoelastic effects in aluminum stripes [15]. Gandhi derived the acoustoelastic effect on Lamb wave dispersion for particular frequency ranges [16].

II. Theoretical Basics

A. Dispersion Relations of Lamb Waves

When a volume wave enters the sample under an oblique angle, the transmitted wave splits in a (quasi-)longitudinal and (quasi-)transversal wave mode travelling through the sample (for angles smaller than the first critical angle). The speed of these wave modes, called partial waves, is determined by the elastic constants of the sample. The transmission angle follows Snell's law. When it hits the other surface the mode is reflected and mode converted resulting again in a splitting in longitudinal and transverse partial waves. If the wavelength of the partial waves fulfills the boundary conditions (stress free surfaces) the modes are hardly attenuated when reflected and the sample becomes a wave guide. The proper wavelength depends on the transmission angle. The partial modes interfere constructively and after some reflections a repetitive pattern is generated (as shown in Fig. 2). The pattern has wave properties and is called Lamb wave. Lamb waves are dispersive – their travelling speed depends on frequency.

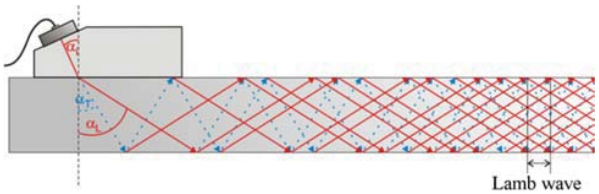

Fig. 2 Schematic representation of Lamb wave generation: Reflection and mode conversion of (quasi-) longitudinal (red) and (quasi) transversal (blue) partial waves lead to a repetitive wave pattern called Lamb wave

Horace Lamb derived analytic equations for the dispersion relation based on Snell's law, the mentioned boundary conditions and Hooke's law:

$$\frac{\tan(\alpha_L h)}{\tan(\alpha_T h)} = -\left(\frac{4k^2\alpha_L\alpha_T}{\left(\alpha_T^2-k^2\right)^2}\right)^{\pm 1}, \alpha_i := \sqrt{\frac{\omega^2}{c_i^2}-k^2},\ i \in \{L,T\} \tag{2}$$

h corresponds to the half thickness of the plate, i represents the mode of the partial wave (L for longitudinal, T for transversal). The exponent $+1$ describes the sound transport of the symmetric and -1 the transport of the antisymmetric Lamb

waves (Fig. 3) traveling with phase velocity c_p, wave number $k = \omega/c_p$ and frequency $f = \omega/2\pi$.

The equation can be solved numerically for known elastic properties (use (1) in (2)), density and plate thickness (Fig. 4). There are infinite solutions sorted by order of occurrence in the frequency spectrum.

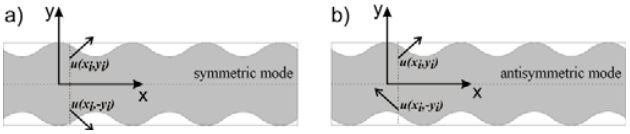

Fig. 3 Schematic representation of the particle deflection u for a) symmetric and b) antisymmetric Lamb modes

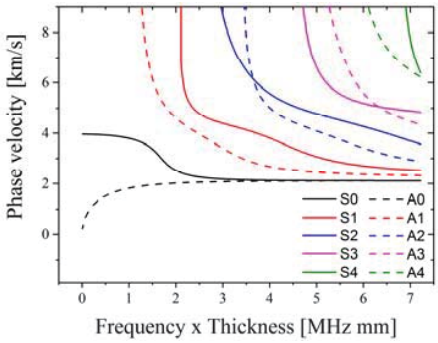

Fig. 4 Dispersion relations of Lamb waves in a copper ribbon. Full lines represent symmetric, dashed lines antisymmetric Lamb modes

B. Acoustoelasticity of Lamb Waves

For a loaded plate with force vector in the plane of the plate, Muir derived an analytic expression for longitudinal and transverse wave speeds traveling at an angle θ with respect to the force vector (but still within the plane):

$$\frac{\Delta c_i}{c_{i,o}} = \sigma\left(K_{i,1}\sin^2\theta + K_{i,2}\cos^2\theta\right) = \sigma K_i(\theta). \quad (3)$$

$c_{i,0}$ represents the wave velocity in the unloaded plate. The constants $K_{i,1}$ and $K_{i,2}$ are functions of the second and third order elastic constants. The index i represents the longitudinal or transversal wave mode. The calculated effective acoustoelastic constant for polycrystalline copper is represented in Fig. 5.

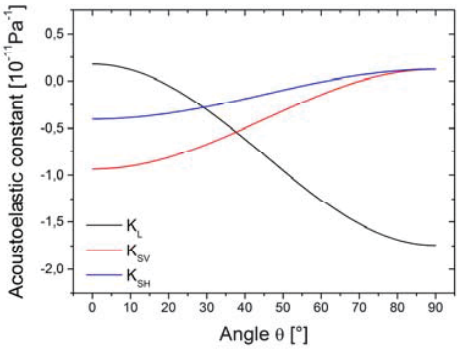

Fig. 5 Angle dependent acoustoelastic model (3) for isotropic copper

Using the angle dependent acoustoelastic constant $K_i(\theta)$ the velocities and directions of the partial waves, as well as the phase velocity of the Lamb wave can be calculated for a given load (acoustoelastic dispersion relations) (Fig. 6).

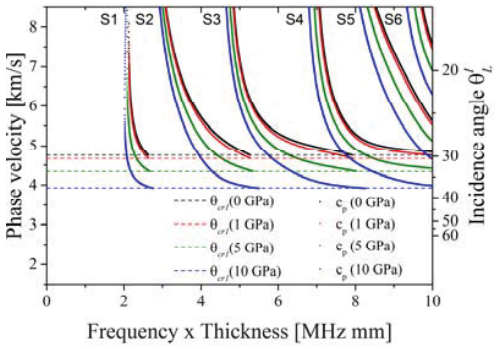

Fig. 6 Theoretical dispersion relations in dependence of the applied load (highly exaggerated to show the influence). Dashed lines represent the first critical angles in the measurement setup

III. Methods

A. Method 1: Dispersion-Based Elastic Constant Characterization:

1. Measurement

For this method, the distance between the transducers and thus the path length of the traveling sound through the ribbon can be varied by a universal testing machine (Fig. 7).

Fig. 7 Schematic setup for method 1

The transducers freely glide over the sample at constant speed v without loading it. A linear frequency chirp is used to excite the ultrasonic waves in the transducer. This way a polychromatic Lamb wave is excited, travels through the sample and is detected by the receiving transducer. The detected signal is bandpass filtered around the center frequency f_i, normalized by Hilbert transformation and saved as a reference. The same signal evaluation procedure is applied for the received signal at all the other transducer positions. The phase relation between the actual and the reference position is evaluated by Lissajous figures (one axis corresponds to the filtered reference time signal, the other axis to the filtered time

signal at current position). Due to the movement of the transducer the phase is constantly changing with a fixed rate $\Delta\varphi/\Delta t$. The phase velocity of the Lamb wave at frequency f_i can be calculated by:

$$c_p(f_i) = \lambda f_i = \frac{\Delta t}{\Delta\varphi_i} 2\pi f_i v = 2\pi f_i \frac{\Delta x}{\Delta\varphi_i} \quad (4)$$

The procedure is repeated for other filter frequencies. The computation is very fast such that multiple frequencies can be evaluated before the next signal is detected. This way the Lamb wave dispersion curves can be evaluated over a wide frequency range within one measurement.

2. Evaluation

In order to evaluate the elastic parameters, the dispersion model (2) is automatically fitted to the measured phase velocities. Fit parameters are (effective) Young's modulus and Poisson's ratio or in terms of partial waves: the longitudinal and transversal velocity. Both are related to each other by (1). The fitting algorithm minimizes the square error χ^2 between the simulated c_{Mod} and measured c_{Meas} phase velocities such that:

$$\chi^2(Y,\nu) = \sum_{i=1}^{n} \left(c_{Mod}(f_i, Y, \nu) c_{Meas}(f_i)\right)^2 \quad (5)$$

For process control in industrial applications the fitting algorithm is too slow on standard computers. Therefore the dispersion relations were stored in and later loaded from a database. The database was built by solving the dispersion relations for various combinations of Young's modulus and Poisson's ratio in a user defined interval (e.g. for Young's modulus in the range from 90 to 140 GPa, Poison's ratio from 0.2 to 0.4) and in a user defined resolution (e.g. 0.1 for Young's modulus and 0.01 for Poisson's ratio). The calculation of the database takes hours but can be applied for future analysis and even different materials, when the density ratio of copper and the different material ρ_{Cu}/ρ_i is used as a scaling factor for Young's modulus (see (1)). By loading the dispersion curves from the database the fitting algorithm is fast (<1s) enough for industrial application (depending on defined parameter range, resolution and number of measured data points).

B. Method 2: Acoustoelasticity of Lamb Waves for Measuring Prestress

1. Measurement

Acoustoelastic changes in wave velocity are very small (typically a few m/s), therefore a more sensitive measurement technique has to be applied. The transducers are located at a fixed distance l to each other such that the sound path length is constant and the samples are tensile loaded by a universal testing machine (Fig. 8).

A linear chirp is used as excitation signal. The measured time signals at different loads F_j and the reference load F_0 are narrowband filtered (at center frequency f). For sufficiently small bandwidth and changes in wave speed the dispersion effect can be neglected. An automatic windowing procedure searches the filtered signal at reference load for a signal part with high signal-to-noise ratio. This signal part is used as reference signal $s_{ref}(f)$. The time signals at loads F_j are filtered similarly $s_j(f)$ and cross-correlated to the reference by:

$$(s_j * s_{ref})(t_0) := \sum_{t_{initial}}^{t_{final}} s_j^*(t) s_{ref}(t + t_0) \quad (6)$$

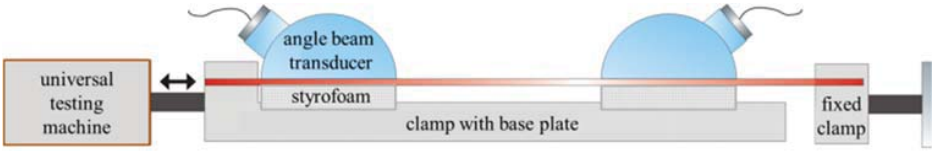

Fig. 8 Schematic setup for method 2

The correlation function $(s_j * s_{ref})(t_0)$ reaches the global maximum when t_0 corresponds to the load induced change in time-of-flight $\Delta TOF(F,f)$. For known transducer distance l the change in (group) velocity Δc_G can be calculated by:

$$\Delta c_G(F,f) = l/\Delta TOF(F,f). \quad (7).$$

For small loads (such that lateral contraction can be neglected) the effective acoustoelastic constant is:

$$K(f) \approx \frac{\Delta TOF(F_j,f)}{TOF_0(F_0,f)} \frac{A}{\Delta F}. \quad (8)$$

TOF_0 represents the time-of-flight at reference load, ΔF is the force difference between actual and reference load and A describes the cross-section area of the sample.

The measuring procedure is automatically repeated for different frequencies such that the frequency dependence of $K(f)$ is determined. In most industrial applications only changes in microstructure are of interest. For this purpose it is not necessary to measure the whole frequency dependence of $K(f)$ in real time. Instead, when investigating a new sample the frequency sweep is only applied once. This sweep is used to identify the most sensitive modes / frequencies. During production only these frequencies are monitored under constant force and temperature. This way the evaluation time is very fast and small microstructural changes can be detected even at high production speeds.

IV. Experiments and Results

A. Sample Preparation

In previous investigations it was found that the most critical influences on the mechanical properties of the ribbon are the annealing process and the mechanical loading after annealing (in subsequent processing, transport or after treatments).

In order to test the developed methods with respect to their applicability in these scenarios the samples were pretreated in the lab to simulate different process conditions. Two types of samples were conditioned: First, unannealed copper ribbons from an interconnector manufacturer were annealed in a rapid thermal processing oven and the annealing times were varied. Afterwards mechanical load tests and microstructural analysis were carried out in order to compare these results to the Lamb wave methods. Second, industrial annealed samples were stressed in a universal testing machine to simulate tensile pre-stress by transport rolls or by stretch forming before soldering.

B. Method 1: Dispersion-Based Elastic Constant Characterization

Method 1 turned out to be very robust with respect to micro-structural changes. In Fig. 9 the measured and automatic fitted dispersion curves are shown for differently annealed copper ribbons. The first minute of annealing drastically influences the course of the dispersion relations. This suggests that especially the beginning of the annealing has high impact on the elastic constants of the ribbon. At longer annealing times the change in dispersion relations is comparatively small.

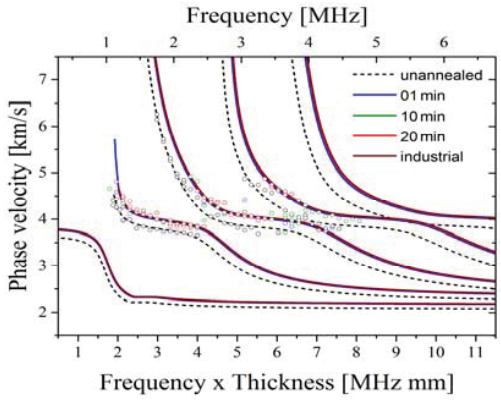

Fig. 9 Measured phase velocities and fitted dispersion curves used to evaluate the effective Young's modulus and Poisson's ratio

The evaluated Young's modulus is plotted versus annealing duration in Fig. 10.

The biggest change in elastic parameters is in fact at the beginning of the annealing process during recrystallization. Grains which were stressed and had a preferred orientation due to the mechanical processes before (drawing and rolling) split up and generate new smaller unstressed grains without preferred direction. As a result, the average grain orientation becomes more isotropic and the effective Young's modulus changes towards the isotropic limit (for copper 123.5 GPa).

After (primary) recrystallization grain growth occurs. The unstressed new grains expand on costs of the remaining pre-stressed grains. The process is slower and therefore the rate of change of Young's modulus is smaller. In Table I, the results are compared to results from tensile testing and micro¬structural analysis.

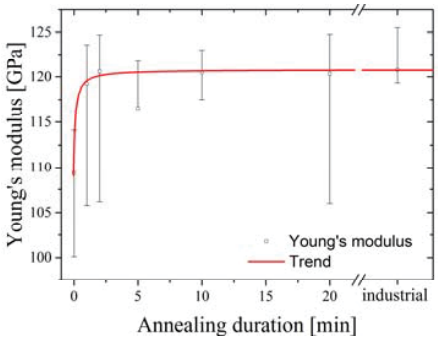

Fig. 10 Young's modulus determined by method 1 in dependence of annealing duration. The error-bars show the theoretical maximum possible error

TABLE I
COMPARISON OF METHODS

Sample	$Y_{US}[GPa]$	$Y_{EBSD}[GPa]$	$Y_{tensile}[GPa]$
Unannealed	116.9 ± 2.3	117.0	106.0 ± 15
Annealed	121.1 ± 2.4	128.9	108.8 ± 15

Young's modulus evaluated with different techniques: Lamb waves (method1) Y_{US}, texture based analysis Y_{EBSD}, tensile testing $Y_{tensile}$

For tensile testing Young's modulus was measured by the slope in the elastic part of the stress-strain diagram. For microstructural analysis Young's modulus was determined by calculating the effective elastic constant for each grain with respect to its orientation (using the orientation from electron backscatter diffraction and the elastic tensor of the copper single crystal). The effective elastic constants of each grain were weighted by their grain size and added up to calculate the effective Young's modulus over the cross-section. The micro-structural results are in good agreement to the ultrasonic results.

Young's moduli determined by tensile testing are significantly smaller. Reasons are the limited stiffness of the testing machine, systematic errors by measuring the cross-section and the much slower loading amplitude. Ultrasonic measurement methods correspond to loading with the speed of sound. So small-scale viscoelasticity effects as creeping or stress-relaxation can be neglected.

Mechanical loading has smaller influence on the elastic modulus therefore this method is not sensitive enough to resolve it adequately. For that reason, the acoustoelastic approach was used for that purpose.

C. Method 2: Acoustoelasticity of Lamb Waves for Measuring Prestress

Method 2 turned out to be very sensitive. But there is no easy systematic variation which can be used to track the annealing duration. This is due to the fact that annealing does not only influence the acoustoelastic constant (which is related to the third order elastic constants) but also the dispersion relations as seen previously (second order elastic constants). This leads to completely different frequency behavior of the acoustoelastic constant and therefore cannot be tracked so easily. As known from the previous paragraph the effect of mechanical pre-stress on the elastic constants is much smaller, so it is better suited for this method. In Fig. 11 the frequency behaviors of the

acoustoelastic constant for the S0 and S1 mode are shown.

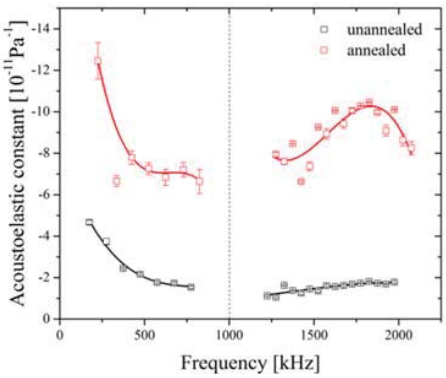

Fig. 11 Acoustoelastic constant in dependence of frequency. Error-bars indicate the measurement precision according to Gaussian error propagation

The influence of the annealing can be seen easily. Furthermore it can be concluded which frequencies are most sensitive for acoustoelastic measurements of the samples: Frequencies with a higher acoustoelastic constant leads to higher changes in time-of-flight for same change in load and therefore to a higher resolution with respect to small microstructural changes.

Annealed and unannealed ribbons were cyclic mechanically loaded and the selected frequency range was investigated (Fig. 12). One loading cycle consists of a tensile load of 20 N for 2 minutes and a stress release to 4 N for 2 minutes.

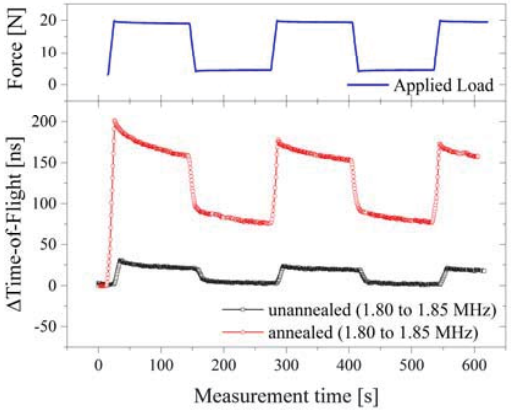

Fig. 12 The measured change in time-of-flight in the first three loading cycles. The permanent offset in TOF for the annealed sample corresponds to plastic deformation. The exponential drop in TOF after loading is a result of stress relaxation and cooling from plastic deformation induced heating (internal friction)

The acoustoelastic constant was evaluated at small forces (< 3 N) in order to check if the method can be used non-destructively. In Fig. 13 it is shown how the acoustoelastic constant changes with increasing load cycles.

The acoustoelastic constant is drastically reduced during the first loading cycle. This is a result of reorientation of the grains toward tensile direction. In the following cycles, the grains are already reoriented such that the remaining effect is much smaller. Furthermore, it is observable that the acoustoelastic constant changes much less for the unannealed ribbon. Here, the grains were already oriented due to the prior mechanical processing steps therefore the mechanical loading leads to smaller grain reorientation. Tracking the acoustoelastic constant for annealed ribbons seems to be promising for measuring small mechanical pre-stress.

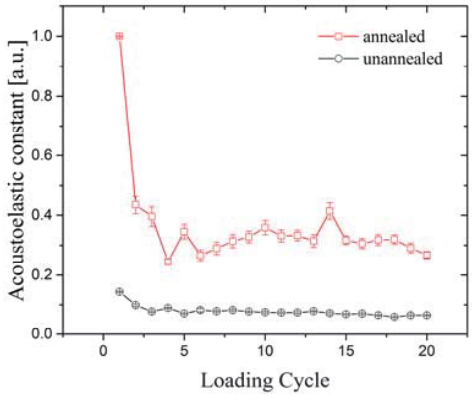

Fig. 13 The change of the acoustoelastic constant with increasing loading cycles. The first cycle induces significant plastic deformation in the annealed sample, the reorientation of the grains lead to a remarkable reduction of the acoustoelastic constant

V. Conclusion

In this paper two Lamb wave methods were shown for potential use in inline production process surveillance and quality assurance. The first method was based on the dispersion relations of Lamb waves and their dependence on the elastic constants. This method is suited for elastic module characterization of the samples. It is possible to monitor the annealing process especially at the beginning. For detecting small differences at longer annealing times the method is less suited since the change in grain orientation and thus the change in modulus is comparably small. Small mechanical pre-stress can also not be detected for the same reasons. Here, the second presented method based on the acoustoelasticity of Lamb waves complements the first. It is not suited for large microstructural changes, since in these cases the dispersion relation change as well and overlay the effect of the acoustoelastic constant. But, small microstructural changes such as mechanical loading can be detected easily by this method. A combination of both methods could be useful tools for production process control.

Acknowledgements

The authors thank the German Federal Ministry for Economic Affairs and Energy for financial support of the project “LAURA" (project no. 0325716B) and “Wuestenmodul” (project no. 03FH014IX4). Special thank goes to Stefan Handrick for experimental support.

REFERENCES

[1] J. Krautkraemer and H. Krautkraemer, *Werkstoffprüfung mit Ultraschall*. Springer Berlin Heidelberg, Berlin and Heidelberg, 5. edition.
[2] H. Lamb, "On waves in an elastic plate," Royal Society of London Proceedings, 1917.
[3] B. A. Auld, *Acoustic fields and waves in solids*, Vol. 2. R.E. Krieger, Malabar, 2. Edition, 1990.
[4] W. P. Rogers, "Elastic property measurement using rayleigh-lamb waves," Research in Nondestructive Evaluation, 1995, 6(4):185–208.
[5] C. Potel et al., "Lamb wave attenuation in a rough plate," Journal of Applied Physics, 104(7):074908, 2008.
[6] B. Pavlakovic et al., "Disperse: A general purpose program for creating dispersion curves," In Thompson, D. O. und Chimenti, D. E., editors, Review of Progress in Quantitative Nondestructive Evaluation, Springer US, Boston and MA, 1997, pp. 185–192.
[7] P. Bocchini, A. Marzani, and E. Viola, "Graphical user interface for guided acoustic waves," Journal of Computing in Civil Engineering, 25(3):202–210, 2011.
[8] K. Vignesh et al., "Non-destructive evaluation of elastic modulus in metals using lamb wave technique," The e-Journal of Nondestructive Testing, 2015, 20(6).
[9] D. S. Hughes and J. L. Kelly, "Second-order elastic deformation of solids," Phys. Rev., 92:1145–1149, 1953.
[10] F. D. Murnaghan, "Finite deformations of an elastic solid," American Journal of Mathematics, 59(2):235–260, 1937.
[11] R. A. Toupin and B. Bernstein, "Sound waves in deformed perfectly elastic materials. acoustoelastic effect," The Journal of the Acoustical Society of America, 33(2), 1961.
[12] D. D. Muir, "One-Sided Ultrasonic Determination of Third Order Elastic Constants using Angle-Beam Acoustoelasticity Measurements," PhD thesis, Georgia Institute of Technology, Atlanta and Georgia, 2009.
[13] R. Meier, "Influences of stress and temperature on the time-of-flight of ultrasound in solid matter," Master's thesis, Universität Leipzig, Leipzig, 2008.
[14] K. S. Tarar et al., "Stress detection with guided acoustic ultrasonic waves by non-linear elastic and geometric effects," In Proceedings of SPIE - The International Society for Optical Engineering, SPIE Proceedings, pages 729518–1 – 729518–8. SPIE, 2009.
[15] U. Amjad et al., "Determination of the stress dependence of the velocity of lamb waves in aluminium plates," In Proceedings of SPIE - The International Society for Optical Engineering, SPIE Proceedings, pages 798410–1 – 798410–9. SPIE, 2011.
[16] N. Gandhi, "Determination of Dispersion Curves for Acoustoelastic Lamb Wave Propagation," PhD thesis, Georgia Institute of Technology, Atlanta and Georgia, 2010.